Journal of Medicinal Chemistry Article

J. Med. Chem. **2010,** *53,* 1347–1356 **1347**
DOI: 10.1021/jm901667k

Synthesis and Biological Evaluation of Triazol-4-ylphenyl-Bearing Histone Deacetylase Inhibitors as Anticancer Agents

Rong He,[†,§] Yufeng Chen,[†,§] Yihua Chen,[†] Andrei V. Ougolkov,[‡,∥] Jin-San Zhang,[‡] Doris N. Savoy,[‡] Daniel D. Billadeau,*[,‡] and Alan P. Kozikowski*[,†]

[†]*Drug Discovery Program, Department of Medicinal Chemistry and Pharmacognosy, University of Illinois at Chicago, 833 South Wood Street, Chicago, Illinois 60612 and* [‡]*Division of Oncology Research, Schulze Center for Novel Therapeutics, College of Medicine, Mayo Clinic, 19-254 Gonda, 200 First Street SW, Rochester, Minnesota 55905.* [§]*These authors contributed equally.* [∥]*Present address: Department of Pathology, Northwestern University, Chicago, Illinois 60611.*

Received November 11, 2009

Our triazole-based histone deacetylase inhibitor (HDACI), octanedioic acid hydroxyamide[3-(1-phenyl-1*H*-[1,2,3]triazol-4-yl)phenyl]amide (**4a**), suppresses pancreatic cancer cell growth in vitro with the lowest IC_{50} value of 20 nM against MiaPaca-2 cell. In this study, we continued our efforts to develop triazol-4-ylphenyl bearing hydroxamate analogues by embellishing the terminal phenyl ring of **4a** with different substituents. The isoform inhibitory profile of these hydroxamate analogues was similar to those of **4a**. All of these triazol-4-ylphenyl bearing hydroxamates are pan-HDACIs like SAHA. Moreover, compounds **4h** and **11a** were found to be very effective inhibitors of cancer cell growth in the HupT3 (IC_{50} = 50 nM) and MiaPaca-2 (IC_{50} = 40 nM) cancer cell lines, respectively. Compound **4a** was found to reactivate the expression of CDK inhibitor proteins and to suppress pancreatic cancer cell growth in vivo. Taken together, these data further support the value of the triazol-4-ylphenyl bearing hydroxamates in identifying potential pancreatic cancer therapies.

Introduction

Epigenetic alterations involve regulation of gene expression and are critical to the pathogenesis of many diseases including cancer and various neurodegenerative diseases.[1,2] Histone modification is one of the molecular mechanisms that mediate epigenetic phenomena.[3] Two types of enzymes, histone acetyltransferases (HATs[a]) and histone deacetylases (HDACs), control the acetylation of histones. In general, HATs function to acetylate lysine groups in nuclear histones, resulting in neutralization of the charges on the histones and a more open, transcriptionally active chromatin structure, while HDACs function to deacetylate and suppress transcription. A shift in the balance of acetylation on chromatin may result in changes in the regulation of patterns of gene expression.[4] HDAC inhibitors (HDACIs) represent a class of molecularly targeted agents that can modulate epigenetic changes to histone proteins and thereby counteract aberrant gene expression. HDACIs can be classified into structural classes, including short chain fatty acids, small-molecule hydroxamates,[5] cyclic peptides,[2] benzamides,[6] thiol-based compounds,[7] ketones,[8] and other hybrid compounds (Figure 1). A number of HDACIs such as (*E*)-(1*S*,4*S*,10*S*,21*S*)-7-[(*Z*)-ethylidene]-4,21-diisopropyl-2-oxa-12,13-dithia-5,8,20,23-tetraazabicyclo-[8.7.6]tricos-16-ene-3,6,9,19,22-pentone (FR901228)[2] have now reached clinical trials, and suberoylanilide hydroxamic acid (SAHA, **1a**) is marketed by Merck for use in cutaneous T-cell lymphoma (CTCL).[9] Published work on the use of HDACIs in inflammatory disease,[10] neurodegeneration,[11] heart disease,[12] and protozoan infections[13] reflects the growing recognition that HDACIs might serve as therapeutic interventions for diseases other than cancer.

There are 11 HDAC isoforms identified that operate through zinc-dependent mechanisms.[14] These include the class I HDACs 1, 2, 3, and 8, class II that includes 4, 5, 6, 7, 9, and 10, and class IV that contains HDAC 11. Class III enzymes are HDACs in yeast and include the SIRTs (sirtuins) or Sir2- related proteins, which are NAD-dependent HDACs.[15] Most class I HDACs are subunits of multiprotein nuclear complexes that are crucial for transcriptional repression and epigenetic landscaping. A variety of data suggest that HDAC 1 plays an important role in tumorigenesis,[16] and therefore, class I inhibitors are being sought for use as anticancer drugs. Class II HDACs regulate cytoplasmic processes or function as signal transducers that shuttle between the cytoplasm and the nucleus. The class IV enzyme HDAC 11 is poorly understood compared to other HDAC isoforms, and recently it has been found to negatively regulate the expression of the gene encoding interleukin 10 (IL-10) in antigen-presenting cells.[17] HDACs of class I are expressed in most cell types, whereas the expression pattern of class II HDACs is more tissue-restricted. For example, HDACs 4 and 5 are highly expressed in cardiomyocytes and play a role in

*To whom correspondence should be addressed. For D.D.B.: phone, 507-266-4334; fax, 1-507-266-5146; e-mail, Billadeau.Daniel@mayo.edu. For A.P.K.: phone, 312-996-7577; fax, 312-996-7107; e-mail, kozikowa@uic.edu.

[a]Abbreviations: HDAC, histone deacetylase; HDACI, histone deacetylase inhibitor; HAT, histone acetyltransferase; ZBG, zinc binding group; SAHA, suberoylanilide hydroxamic acid; TSA, trichostatin A; CTCL, cutaneous T-cell lymphoma; NAD, nicotinamide adenine dinucleotide; CDK, cyclin-dependent kinase; DNA, Deoxyribonucleic Acid; TLC, thin-layer chromatography; MTT, 3-[4,5-dimethylthiazol-2-yl]2,5-diphenyltetrazolium bromide.

Published on Web 01/07/2010

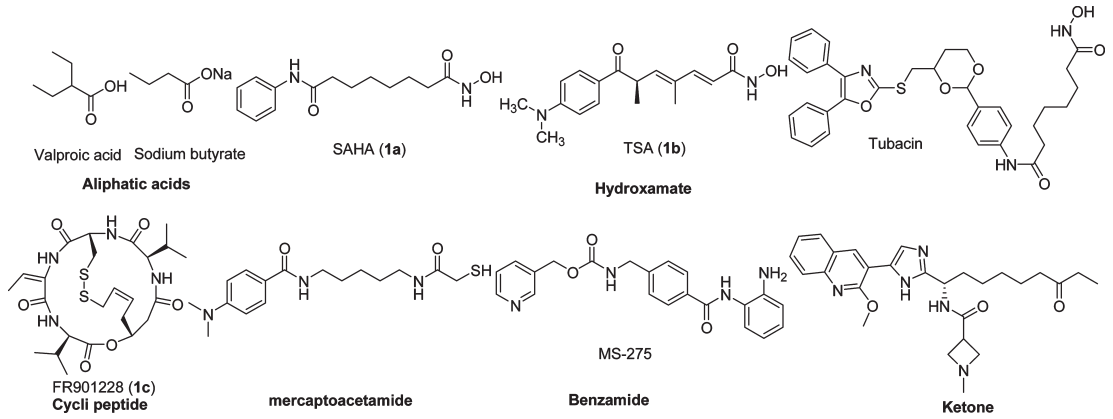

Figure 1. Classes of HDACIs.

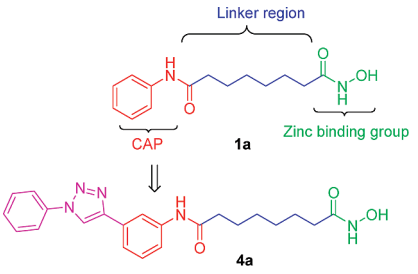

Figure 2. Functional domains of HDACIs.

hypertrophy.[18] HDACs 4, 8, and 9 are expressed to a greater extent in tumor tissues.[19] High expression level of HDAC 11 transcripts is limited to kidney, heart, brain, skeletal muscle, and testis, while the class II enzyme, HDAC 6, is expressed in most neurons.[20] Understanding precise roles of HDAC isoforms will expand our understanding of the connections between individual HDAC isoform and pathophysiology as well as guide the development of selective HDACIs as strategic therapeutic agents that elicit fewer undesirable side effects.

Classical HDACIs have three chemical domains, each with a specific function relating to the structure of the enzyme. Figure 2 shows the structure and functional domains of SAHA (**1a**), which includes a zinc binding group (ZBG), a linker region, and a surface recognition domain (cap). Understanding the mechanism of HDAC is beneficial for a study of the interactions between HDACIs and the enzyme. The active site of classes I, II, and IV HDACs is found within a highly conserved catalytic domain containing a divalent zinc cation that is coordinated to both histidine and aspartate residues. Deacetylation of the HDAC substrates occurs through attack by a water molecule that is activated through interaction with this zinc cation coupled with deprotonation through a histidine−aspartate charge-relay system. To date, X-ray cocrystallographic information is available for HDACs 4, 7, and 8, in complex with several different inhibitors including SAHA (**1a**), TSA (**1b**), and others.[21] These crystal structures of the HDAC enzymes and the derived homology models provide valuable information in the design of selective HDACIs. We have been able to obtain varying degrees of isozyme selectivity for the HDACIs through chemical manipulations of the CAP region in concert with the ZBG. For example, we have reported that certain mercaptoacetamide-based HDACIs show inherent selectivity for HDAC 6 versus HDAC 1 and that some of these thiol-based agents are able to provide robust neuroprotection in the homocysteic acid model of oxidative stress.[7,22] Moreover, one of these thiol-based HDACIs was found to reduce neuronal cell loss in a rodent model of traumatic brain injury.[23] We also have identified HDACIs containing a phenylisoxazole as the cap group that possess excellent selectivity and picomolar potency for HDAC 6.[24] In other studies, we have reported a series of trazolylphenyl-based HDACIs for which we demonstrated that modifications to the cap region were able to alter selectivity for HDAC 1 versus HDAC 6.[25] Preliminary studies of the anticancer and antimalarial activity of these triazol-4-ylphenyl bearing hydroxamates (**4a**) suggested that these compounds were worth further structural optimization (Figure 2). In this paper, we present additional details of the structure−activity relationship (SAR) studies of the parent compound **4a** that focus on steric and/or electronic effects on CAP region. The biological studies presented here include HDAC isoform profiling and cell-based antiproliferative screening toward pancreatic cancer cell lines of all the newly synthesized triazolylphenyl-based HDACIs, together with cell-cycle dysregulation, induction of CDK inhibitor proteins, and in vivo xenograft study of **4a**.

Results and Discussion

Chemistry. The copper-catalyzed [3 + 2]-cycloaddition of acetylene **1** with azides **2a**−**l** provided the 1,4-disubstituted triazoles **3a**−**l**, in analogy to work previously reported by us.[26] The terminal ester groups of compounds **3a**−**j** and **3l** were then treated with KOH/NH_2OH in methanol to afford the final hydroxamates **4a**−**j** and **4l** (Scheme 1).

As shown in Scheme 2, the synthesis of the reversed 1,4-disubstituted triazoles **11a** and **11b** started from the mono-Boc protected 1,3-phenyldiamine **5**. Compound **6** was prepared by a coupling reaction between compound **5** and suberic acid monomethyl ester in the presence of $POCl_3$ and pyridine, which was further converted to compound **7** by deprotection of the Boc group in trifluoroacetic acid. The diazotization of the resulting aniline **7** with NaN_3 provided the phenylazide **8**. The cycloaddition of compound **8** with phenylacetylene or cyclohexylacetylene provided the reversed triazoles **10a** and **10b**, respectively.[26] Treating **10a** and **10b** with KOH/NH_2OH in methanol gave the desired hydroxamates **11a** and **11b** (Scheme 2).

HDAC Isoform Inhibition Assay. The inhibitory effects of compounds **4b**−**j**, **4l**, **11a**,**b**, and **12a** on HDAC activity were determined by using a fluorescence-based assay as described before.[7] The data are presented as IC_{50} values in Table 1.

Scheme 1. Synthesis of Ligands **4a**−**j** and **4l**[a]

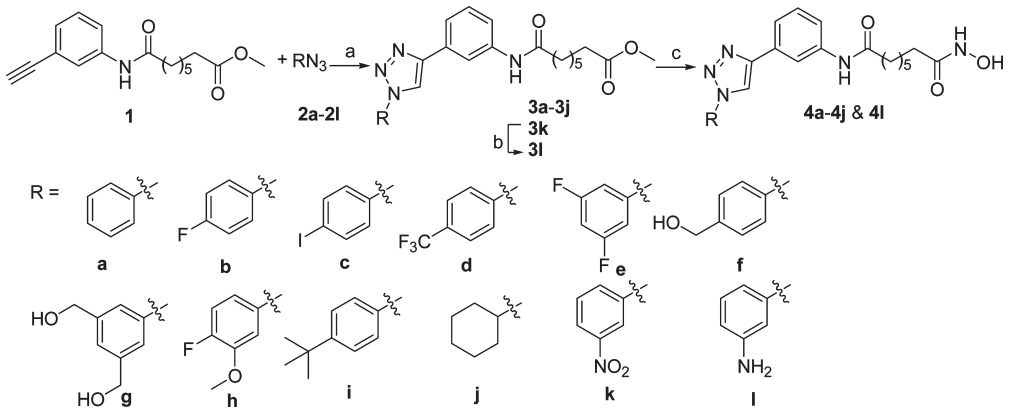

[a] Reagents and conditions: (a) copper sulfate pentahydrate, sodium ascorbate, azides **2a**−**j**, room temp; (b) H_2, 10% Pd−C, room temp, 4 h; (c) NH_2OH, KOH, room temp.

Scheme 2. Synthesis of Ligands **11a** and **11b**[a]

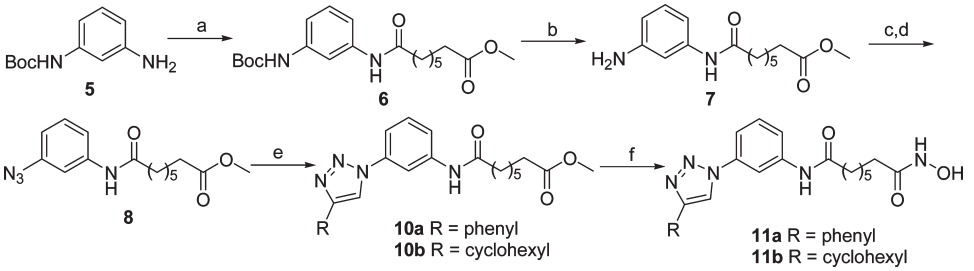

[a] Reagents and conditions: (a) suberic acid monomethyl ester, $POCl_3$, pyridine, 0 °C; (b) TFA, 0 °C; (c) HOAc, $NaNO_2$, 0 °C; (d) NaN_3, 0 °C; (e) copper sulfate pentahydrate, sodium ascorbate, phenylacetylene (**9a**) or cyclohexylacetylene (**9b**), room temp; (f) NH_2OH, KOH, room temp.

Table 1. HDAC Isoform Inhibitory Activity (IC_{50}, nM) of the Triazole-Based Ligands

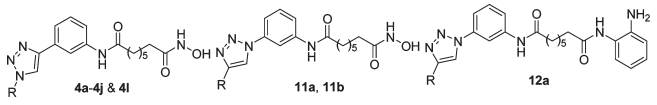

			IC_{50} [nM][a]					
compd	ClogP[b]	R	HDAC 1	HDAC 2	HDAC 3	HDAC 8	HDAC 10	HDAC 6
1a	1.44		96	282	17	2290	72	14
1b	2.23		4	14	2	1380	5	1
4a	2.39	Ph	18 ± 2	63.9 ± 12.5	7.2 ± 0.7	2780 ± 470	27.7 ± 1.9	9.6 ± 0.6
4b	2.59	4-F-Ph	31.9 ± 2.9	60 ± 10	18.1 ± 1.9	12000 ± 800	32.8 ± 5.0	8.4 ± 1.8
4c	3.55	4-I-Ph	8.0 ± 0.6	24.6 ± 0.8	3.0 ± 0.1	> 30000	10.7 ± 0.7	2.2 ± 0.1
4d	3.35	4-CF_3-Ph	8.7 ± 0.3	28.5 ± 1.0	3.4 ± 0.2	5220 ± 390	14.5 ± 0.6	2.9 ± 0.1
4e	2.79	3,5-F,F-Ph	5.3	NA[c]	1.4	NA[c]	NA[c]	1.7
4f	1.47	4-$OHCH_2$-Ph	3.04	NA[c]	1.66	NA[c]	NA[c]	7.6
4g	0.96	3,5-$OHCH_2$-,$OHCH_2$-Ph	5.7 ± 0.2	27.8 ± 0.7	3.3 ± 0.2	1320 ± 80	5.8 ± 0.1	1.9 ± 0.1
4h	2.37	4-F-,3-CH_3O-Ph	5.06	NA[c]	3.39	NA[c]	NA[c]	3.85
4j	3.44	cyclohexyl	8.6 ± 0.2	27.5 ± 1.0	3.7 ± 0.1	1190 ± 490	9.8 ± 0.1	3.3 ± 0.1
4l	1.47	4-NH_2-Ph	1.01	NA[c]	1.55	NA[c]	NA[c]	2.52
11a	2.39	Ph	4.6 ± 0.1	25.1 ± 2.0	2.8 ± 0.2	4180 ± 390	6.8 ± 0.3	3.1 ± 0.2
11b	3.44	cyclohexyl	12.1 ± 0.4	48.2 ± 2.3	5.3 ± 0.5	2750 ± 120	16.6 ± 0.5	4.3 ± 0.5
12a	3.85	Ph	> 30000	> 30000	122 ± 9	> 30000	> 30000	> 30000

[a] The isoform inhibition was tested at Nanosyn, http://www.nanosyn.com. [b] CLogP (KOWWIN) were calculated from http://146.107.217.178/lab/alogps/start.html. [c] NA = not assayed.

TSA (**1b**) was used as a positive control. The inhibitory data for SAHA (**1a**) are also presented for comparison.

The IC_{50} values of the newly synthesized hydroxamate HDACIs are similar to those of the lead compound **4a**. Most of these analogues inhibit HDACs 1, 3, 10, and 6 in the nanomolar range and are slightly less potent at HDAC 2 while showing only micromolar activity against HDAC 8. No significant isozyme selectivity was observed in this set of structures (**4a**−**j**, **4l**, and **11a**,**b**). Introduction of different substituents on the terminal phenyl ring of **4a** increased its

Table 2. Triazole-Based HDACIs Suppress Growth of Pancreatic Cancer Cells

	inhibition of pancreatic cancer cell lines (IC_{50}, μM)				
compd	BxPC-3	Hup T3	Mia Paca-2	Panc04.03	SU 86.86
SAHA (**1a**)	5	0.8	1.1	1.2	1.3
4a	0.4	0.2	0.02	> 0.5	0.8
4b	1	0.1	0.1	0.2	0.6
4c	1.1	1.4	2.33	2.34	7.7
4d	0.9	0.4	0.9	1.9	1.5
4e	1.2	0.4	0.8	2.03	1.7
4f	1	0.2	0.2	1	1
4g	29	7	14	27	37
4h	0.2	0.05	0.1	0.1	1
4i	1.2	0.5	0.6	0.7	1.2
4j	4	0.4	0.1	0.5	0.1
4l	1.2	0.55	0.88	0.36	1.45
11a	0.9	0.1	0.04	0.1	0.2
11b	2	0.4	0.1	0.5	0.9
12a	> 50	> 50	> 50	> 50	32

HDAC inhibitory activity, although these modifications failed to influence the levels of HDAC isozyme selectivity. For example, compound **4d** with an electron withdrawing *p*-trifluoro group on the terminal phenyl ring was 2- to 3-fold more potent than compound **4a** against HDACs 1, 2, 3, 10, and 6 while it was 1.9-fold less potent than compound **4a** in HDAC 8. Comparison of inhibitors **4l** and **4a** shows that the addition of a *p*-amino group on the terminal phenyl ring of **4a** also leads to an increase in inhibitory activity against HDAC 1 (18-fold), HDAC 3 (5-fold), and HDAC 6 (4-fold). Replacement of the terminal phenyl ring of **4a** with a cyclohexyl group as in **4j** led to a 2- to 3-fold increase in potency against all tested HDACs (HDACs 1, 2, 3, 8, 10, and 6). The reversed 1,4-disubstituted triazole **11a** was more potent than compound **4a** against HDACs 1, 2, 3, 10, and 6. The other reversed 1,4-disubstituted triazole **11b** was slightly less potent than compound **4j** in all tested HDACs. Compound **12a** has previously been reported by us, and it represents a benzamide-based HDACI that selectively inhibits HDAC 3 over the other tested HDAC isoforms.[27]

Triazole-Based HDACIs Reactivate Expression of CDK Inhibitors and Suppress Growth of Pancreatic Cancer Cells. Pancreatic cancer is the fourth leading cause of cancer death in the U.S. and essentially remains an incurable disease with the incidence nearly equaling the mortality. Altered HDAC activity is seen to be associated with many cancers, validating HDACs as promising targets for cancer therapy. In fact, treatment of pancreatic cancer cells with the broad spectrum class I/II HDACI, SAHA (**1a**), leads to up-regulation of p21, growth inhibition, and an increase in gemcitabine-induction of apoptosis.[28] Furthermore, SAHA (**1a**) was found to enhance the antiproliferative effect of a DNA methylation inhibitor, 5-aza-2′-deoxycytidine, on pancreatic cancer cells.[29]

In continuation of our efforts to develop HDACIs as antipancreatic cancer therapeutics, we assayed these newly synthesized triazoles (**4b**−**j**, **4l**, **11a**,**b**, and **12a**) against a panel of pancreatic cancer cell lines, which consisted of BxPC-3, HupT3, MiaPaca-2, Pan04.03, and SU86.86 cell lines. The effect of the tested analogues on cancer cell growth was measured by MTT assay, and the IC_{50} values obtained against these cell lines are summarized in Table 2. The data for SAHA (**1a**) and compound **4a** are provided for comparison purposes. As is apparent from the data in Table 2, the majority of our HDACIs (**4a**−**f**, **4h**−**j**, **4l**, and **11a**,**b**) have

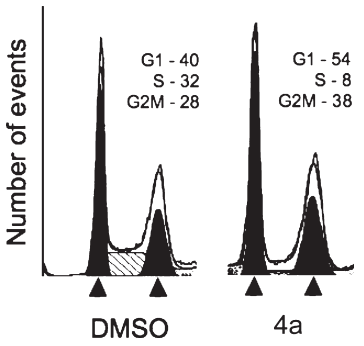

Figure 3. Effect of compound **4a** on cell cycles. Panc04.03 cells were treated with vehicle (DMSO) or compound **4a** (5 μM) for 24 h. Cells were subsequently harvested and stained with propidium iodine, and cell cycle was analyzed using flow cytometry. The percentage of cells in G1, S, and G2M is shown.

IC_{50} values equal to or less than those of SAHA (**1a**) with the exception of compounds **4g** and **12a**. Compound **4a** was the most active analogue against the MiaPaca-2 cells line with an IC_{50} value of 20 nM. Generally, compound **4a** was a more effective inhibitor of cancer cell growth than compounds 4c−**g**, **4i**−**l**, **11b**, and **12a**. Moreover, compounds **4h** and **11a** were very effective inhibitors of cancer cell growth in the HupT3 (IC_{50} = 50 nM) and MiaPaca-2 (IC_{50} = 40 nM) cancer cell lines, respectively. On the other hand, compound **4g** was able to only moderately inhibit cell growth in the five pancreatic cancer cell lines. The weak inhibitory activity of compound **4g** against the different pancreatic cancer cell lines might be due to its polarity, as it has a lower ClogP value than those of the other triazole analogues. Correlative studies reporting aberrant expression and/or localization of HDAC 3 in various tumors imply an important role of HDAC 3 in carcinogenesis.[30] HDAC 3 is also reported to be a repressor of ULBPs expression in epithelial cancer cells[31] and to be linked to the cell cycle machinery of MiaPaCa2 cells.[32] While **12a** exhibits HDAC 3 selectivity, its poor growth inhibition may be due to its poorer HDAC inhibitory activity.

To directly examine the effect on proliferation, we performed cell cycle analysis on Panc04.03 cells, which were treated for 24 h with either vehicle alone or compound **4a**, the best HDACI in this series. Compared to the vehicle-treated Panc04.03 cancer cells, which show a cell cycle profile consistent with rapidly proliferating cells, Panc04.03 cancer cells treated with compound **4a** demonstrate a loss of S-phase cells and an increase in the percentage of cells in G1 (Figure 3). The increase in G2/M cells in the cells treated with compound **4a** may reflect additional effects on microtubule stabilization, which is frequently associated with increases in acetylated α-tubulin, which is deacetylated by HDAC 6.

One of the key features of HDACIs is that they have the capability of reactivating tumor suppressor genes in cancer cells that can inhibit proliferation and survival of the cancer cells. The CDK inhibitor protein p21 is frequently epigenetically silenced in tumor cells, and reactivation of this protein can cause cell cycle arrest and induce senescence and apoptosis in cancer cells. We therefore examined whether treatment of the BXPC-3 cell line with compound **4a** would lead to the expression of p21 (Figure 4). Indeed, although p21 protein levels are nearly undetectable in the BXPC-3 cell line treated with vehicle (DMSO) alone, the addition of

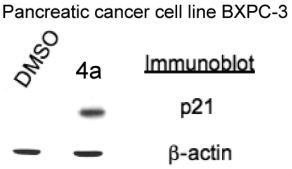

Figure 4. HDACI **4a** reactivates expression of the CDK inhibitor p21 in BXPC3 pancreatic cancer cells. The pancreatic cancer cell line BXPC3 was treated with vehicle (DMSO) or compound **4a** (5 μM) for 18 h. Cell lysates were prepared, separated by SDS−PAGE, transferred to PVDF membrane, and immunoblotted as indicated.

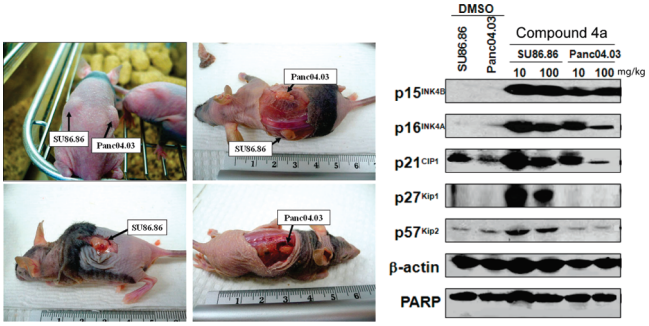

Figure 5. CDK inhibitors are re-expressed in SU86.86 and Panc04.03 mouse xenograft tumors upon treatment with HDACI **4a**. (A) Female athymic nude mice (8−10 weeks old) were inoculated subcutaneously with 3×10^6 Su86.86 (left flank) and Panc04.03 (right flank) pancreatic cancer cells mixed with Matrigel (BD Biosciences). Two weeks after injection, tumors were size-matched and mice were randomized into three treatment groups: (a) control DMSO, four mice; (b) compound **4a** (10 mg/kg), four mice; (c) compound **4a** (100 mg/kg), four mice. Established SU86.86 and Panc04.03 xenografts (tumor volume 150−200 mm^3) were treated by ip injections with diluent (50 μL of DMSO) or compound **4a** (10 and 100 mg/kg; every 12 h for 48 h). (B) Tumor proteins were extracted from fresh tumor tissues taken from mouse, separated by SDS−PAGE (50 μg/well), transferred to polyvinylidene difluoride membrane, and probed with the indicated antibodies.

compound **4a** resulted in an increased expression of p21. As shown in Figure 5, expression of CDK inhibitors p15, p16, p21, p27, and p57 was reactivated in mouse xenograft tumors upon treatment with compound **4a**.

Conclusion

Substituted 1-aryl-1*H*-[1,2,3]triazolylphenyl-based analogues of compound **4a** were designed, synthesized, and profiled for their HDAC isoform selectivity and antiproliferative activities against pancreatic cell lines. The preliminary in vivo evaluation of compound **4a** on established pancreatic tumor cell line xenografts was also determined. We found that compound **4a** could reactivate expression of CDK inhibitor proteins as well as suppress pancreatic cancer cell growth in vivo. The fluorinated analogues **4b**, **4e**, **4h** of compound **4a** may have potential in PET imaging studies. Taken together, our current findings strongly suggest that compound **4a** and its related compounds may ultimately be useful in various combination treatment strategies for pancreatic cancer.

Experimental Section

Chemistry. ^{1}H NMR and ^{13}C NMR spectra were recorded on a Bruker spectrometer at 300/400 MHz and 75/100 MHz, respectively, with TMS as an internal standard. Standard abbreviation indicating multiplicity was used as follows: s = singlet, d = doublet, t = triplet, q = quartet, quin = quintuplet, m = multiplet, and br = broad. HRMS experiment was performed on a Q-TOF-2TM (Micromass) instrument. TLC was performed with Merck 250 mm $60F_{254}$ silica gel plates. Preparative TLC was performed with Analtech 1000 mm silica gel GF plates. Column chromatography was performed using Merck silica gel (40−60 mesh). HPLC was carried out on Agilent 1100 HPLC system with a Synergi 4 μm Hydro-RP 80A column, with detection at 254 on a variable wavelength detector G1314A. Method 1 consisted of the following: flow rate = 1.4 mL/min; gradient elution over 20 min from 30% CH_3OH-H_2O to 100% CH_3OH with 0.05% TFA. Method 2 consisted of the following: flow rate = 1.4 mL/min; gradient elution over 20 min, from 10% CH_3OH-H_2O to 100% CH_3OH with 0.05% TFA. Method 3 consisted of the following: flow rate = 1.4 mL/min; gradient elution over 20 min from 100% H_2O to 100% CH_3OH with 0.05% TFA.

7-{3-[1-(4-Fluoro-phenyl)-1*H*-[1,2,3]triazol-4-yl]phenylcarbamoyl}heptanoic Acid Methyl Ester (3b). In a mixture of **1** (100 mg, 0.34 mmol) and 1-azido-4-fluorobenzene (**2b**, 143 mg, 1.04 mmol) in water and ethyl alcohol (v/v = 1:1, 10 mL), sodium ascorbate (28 mg, 0.14 mmol, dissolved in 1 mL of water) was added, followed by the addition of copper[33] sulfate pentahydrate (17 mg, 0.07 mmol, dissolved in 1 mL of water). The heterogeneous mixture was stirred vigorously overnight at room temperature. The reaction mixture was diluted with EtOAc and washed thoroughly with brine, dried over Na_2SO_4, filtered, and concentrated. The residue was purified by column chromatography on silica gel (hexanes/EtOAc, 1:1) to afford 77 mg (52%) of **3b**. R_f = 0.47 (1:1 hexane/EtOAc). ^{1}H NMR (DMSO-d_6, 400 MHz): δ = 1.30 (br s, 4H), 1.53 (t, J = 8.0 Hz, 2H), 1.58 (t, J = 8.0 Hz, 2H), 2.28−2.34 (m, 4H), 3.57 (s, 3H), 7.40 (t, J = 8.0 Hz, 1H), 7.49 (t, J = 8.0 Hz, 2H), 7.55 (d, J = 8.0 Hz, 1H), 7.59 (d, J = 8.0 Hz, 1H), 8.01−8.04 (m, 2H), 8.26 (s, 1H), 9.24 (s, 1H), 10.02 (s, 1H). ^{13}C NMR (DMSO-d_6, 100 MHz): δ = 24.7, 25.3, 28.6, 28.7, 33.6, 36.7, 51.6, 116.3, 117.0, 117.3, 119.3, 120.3, 120.6, 122.7, 122.8, 129.7, 131.0, 133.6, 140.3, 147.7, 171.8, 173.7.

7-{3-[1-(4-Iodophenyl)-1*H*-[1,2,3]triazol-4-yl]phenylcarbamoyl}heptanoic Acid Methyl Ester (3c). Compound **3c** (yield 38%) was prepared from **1** and 1-azido-4-iodobenzene (**2c**) according to the methodology described for the preparation of compound **3b**. R_f = 0.71 (1:1 hexane/EtOAc). ^{1}H NMR (DMSO-d_6, 300 MHz): δ = 1.28 (br s, 4H), 1.51 (t, J = 6.8 Hz, 2H), 1.58 (t, J = 6.8 Hz, 2H), 2.25−2.33 (m, 4H), 3.55 (s, 3H), 7.38 (t, J = 7.9 Hz, 1H), 7.53 (d, J = 7.5 Hz, 1H), 7.57 (d, J = 7.9 Hz, 1H), 7.79 (d, J = 8.2 Hz, 2H), 7.97 (d, J = 8.2 Hz, 2H), 8.25 (s, 1H), 9.27 (s, 1H), 10.01 (s, 1H). ^{13}C NMR (DMSO-d_6, 75 MHz): δ = 25.1, 25.7, 29.0, 29.1, 34.0, 37.1, 51.9, 116.6, 119.7, 120.3, 121.0, 122.6, 130.1, 131.2, 137.0, 139.4, 140.7, 148.2, 172.1.

7-{3-[1-(4-Trifluoromethylphenyl)-1*H*-[1,2,3]triazol-4-yl]phenylcarbamoyl}heptanoic Acid Methyl Ester (3d). Compound **3d** (yield 51%) was prepared from **1** and 1-azido-4-trifluoromethylbenzene (**2d**) according to the methodology described for the preparation of compound **3b**. R_f = 0.54 (1:1 hexane/EtOAc). ^{1}H NMR (DMSO-d_6, 400 MHz): δ = 1.31(br s, 4H), 1.55 (t, J = 8.0 Hz, 2H), 1.61 (t, J = 8.0 Hz, 2H), 2.35−2.28 (m, 4H), 3.57 (s, 3H), 7.42 (t, J = 8.0 Hz, 1H), 7.58 (t, J = 8.0 Hz, 2H), 8.03 (d, J = 8.0 Hz, 2H), 8.24 (d, J = 8.0 Hz, 2H), 8.30 (s, 1H), 9.42 (s, 1H), 10.03 (s, 1H). ^{13}C NMR (DMSO-d_6, 100 MHz): δ = 24.7, 25.3, 28.6, 28.7, 33.6, 36.7, 51.6, 116.3, 119.5, 120.2, 120.7, 120.8, 125.6, 127.6, 127.7, 128.9, 129.2, 129.8, 130.7, 139.8, 140.4, 148.0, 171.8, 173.7.

7-{3-[1-(3,5-Difluorophenyl)-1*H*-[1,2,3]triazol-4-yl]phenylcarbamoyl}heptanoic Acid Methyl Ester (3e). Compound **3e** (yield 59%) was prepared from **1** and 1-azido-3,5-difluorobenzene (**2e**) according to the methodology described for the preparation of compound **3b**. R_f = 0.55 (1:1 hexane/EtOAc). ^{1}H NMR (DMSO-d_6, 400 MHz): δ = 1.32 (br s, 4H), 1.55 (t, J = 8.0 Hz, 2H), 1.60 (t, J = 8.0 Hz, 2H), 2.28−2.35 (m, 4H), 3.57 (s, 3H), 7.48−7.40 (m, 2H), 7.53−7.59 (m, 2H), 7.85 (d, J = 8.0 Hz, 2H), 8.29 (s, 1H), 9.36 (s, 1H), 10.03 (s, 1H). ^{13}C NMR (DMSO-d_6,

100 MHz): δ = 24.7, 25.3, 28.6, 28.7, 33.6, 36.7, 51.6, 104.1, 104.4, 116.3, 119.5, 120.6, 120.6, 125.8, 129.8, 130.6, 140.4, 148.0, 161.9, 162.1, 171.8, 173.8.

7-{3-[1-(4-Hydroxymethylphenyl)-1*H*-[1,2,3]triazol-4-yl]phenylcarbamoyl}heptanoic Acid Methyl Ester (3f). Compound **3f** (yield 69%) was prepared from **1** and (4-azidophenyl)methanol (**2f**) according to the methodology described for the preparation of compound **3b**. R_f = 0.57 (EtOAc). ^{1}H NMR (DMSO-d_6, 400 MHz): δ = 1.32 (br s, 4H), 1.53 (t, *J* = 8.0 Hz, 2H), 1.60 (t, *J* = 8.0 Hz, 2H), 2.28−2.35 (m, 4H), 3.57 (s, 3H), 4.59 (s, 2H), 5.37 (br s, 1H), 7.40 (t, *J* = 8.0 Hz, 1H), 7.54−7.61 (m, 4H), 7.93 (d, *J* = 8.0 Hz, 2H), 8.26 (s, 1H), 9.23 (s, 1H), 10.01 (s, 1H). ^{13}C NMR (DMSO-d_6, 100 MHz): δ = 24.7, 25.3, 28.6, 28.7, 33.6, 36.7, 51.6, 62.6, 116.3, 119.3, 119.9, 120.2, 120.6, 125.8, 128.0, 129.7, 131.1, 135.6, 140.3, 143.7, 147.6, 171.8, 173.8.

7-{3-[1-(3,5-Bis-hydroxymethylphenyl)-1*H*-[1,2,3]triazol-4-yl]-phenylcarbamoyl}heptanoic Acid Methyl Ester (3g). Compound **3g** (yield 40%) was prepared from **1** and (3-azido-5-hydroxymethylphenyl)methanol (**2g**) according to the methodology described for the preparation of compound **3b**. R_f = 0.26 (EtOAc). ^{1}H NMR (DMSO-d_6, 400 MHz): δ = 1.32 (br s, 4H), 1.54 (t, *J* = 8.0 Hz, 2H), 1.61 (t, *J* = 8.0 Hz, 2H), 2.28−2.35 (m, 4H), 3.58 (s, 3H), 4.62 (s, 4H), 7.38−7.41 (m, 2H), 7.59 (d, *J* = 8.0 Hz, 2H), 7.79 (s, 2H), 8.29 (s, 1H), 9.27 (s, 1H), 10.00 (s, 1H). ^{13}C NMR (DMSO-d_6, 100 MHz): δ = 24.7, 25.3, 28.6, 28.7, 33.6, 36.7, 51.6, 62.8, 116.3, 116.4, 119.3, 119.9, 120.7, 124.6, 129.7, 131.1, 136.9, 140.3, 145.0, 147.6, 171.8, 173.8.

7-{3-[1-(3-Fluoro-4-methoxyphenyl)-1*H*-[1,2,3]triazol-4-yl]-phenylcarbamoyl}heptanoic Acid Methyl Ester (3h). Compound **3h** (yield 70%) was prepared from **1** and 4-azido-2-fluoro-1-methoxybenzene (**2h**) according to the methodology described for the preparation of compound **3b**. R_f = 0.25 (1:1 hexane/EtOAc). ^{1}H NMR (DMSO-d_6, 400 MHz): δ = 1.32 (br s, 4H), 1.54 (t, *J* = 8.0 Hz, 2H), 1.60 (t, *J* = 8.0 Hz, 2H), 2.28−2.34 (m, 4H), 3.57 (s, 3H), 3.93 (s, 1H), 7.38−7.44 (m, 2H), 7.53 (d, *J* = 8.0 Hz, 1H), 7.58 (d, *J* = 4.0 Hz, 1H), 7.79 (d, *J* = 8.0 Hz, 1H), 7.93 (dd, *J* = 12.0 and 4.0 Hz, 1H), 8.25 (s, 1H), 9.20 (s, 1H), 10.01 (s, 1H). ^{13}C NMR (DMSO-d_6, 100 MHz): δ = 24.7, 25.3, 28.6, 28.7, 33.6, 36.7, 51.6, 56.8, 109.1, 109.3, 114.9, 115.0, 116.2, 116.8, 119.3, 120.1, 120.6, 129.7, 130.0, 130.1, 131.0, 140.3, 147.6, 147.7, 150.5, 152.9, 171.8, 173.7.

7-{3-[1-(4-*tert*-Butylphenyl)-1*H*-[1,2,3]triazol-4-yl]phenylcarbamoyl}heptanoic Acid Methyl Ester (3i). Compound **3i** (yield 58%) was prepared from **1** and 1-azido-4-*tert*-butylbenzene (**2i**) according to the methodology described for the preparation of compound **3b**. R_f = 0.47 (1:1 hexane/EtOAc). ^{1}H NMR (DMSO-d_6, 400 MHz): δ = 1.35−1.40 (m, 13H), 1.51 (t, *J* = 8.0 Hz, 2H), 1.60 (t, *J* = 8.0 Hz, 2H), 2.28−2.35 (m, 4H), 3.57 (s, 3H), 7.40 (t, *J* = 8.0 Hz, 1H), 7.56 (d, *J* = 8.0 Hz, 1H), 7.60−7.64 (m, 3H), 7.88 (d, *J* = 8.0 Hz, 2H), 8.25 (s, 1H), 9.20 (s, 1H), 10.01 (s, 1H). ^{13}C NMR (DMSO-d_6, 100 MHz): δ = 24.7, 25.3, 28.6, 28.7, 31.4, 33.6, 34.9, 36.7, 51.6, 116.3, 119.3, 119.9, 120.1, 120.7, 125.8, 127.0, 129.7, 131.1, 134.7, 140.3, 147.6, 151.7, 171.8, 173.7.

7-[3-(1-Cyclohexyl-1*H*-[1,2,3]triazol-4-yl)phenylcarbamoyl]-heptanoic Acid Methyl Ester (3j). Compound **3j** (yield 45%) was prepared from **1** and azidocyclohexane (**2j**) according to the methodology described for the preparation of compound **3b**. R_f = 0.30 (1:1 hexane/EtOAc). ^{1}H NMR (DMSO-d_6, 400 MHz): δ = 1.20−1.32 (m, 5H), 1.40−1.60 (m, 6H), 1.68 (d, *J* = 12.0 Hz, 1H), 1.79−1.85 (m, 4H), 2.11 (d, *J* = 12.0 Hz, 2H), 2.27−2.32 (m, 4H), 3.57 (s, 3H), 4.50 (t, *J* = 8.0 Hz, 1H), 7.33 (t, *J* = 8.0 Hz, 1H), 7.45 (d, *J* = 8.0 Hz, 1H), 7.54 (d, *J* = 8.0 Hz, 1H), 8.14 (s, 1H), 8.56 (s, 1H), 9.95 (s, 1H). ^{13}C NMR (DMSO-d_6, 100 MHz): δ = 24.7, 25.0, 25.1, 25.3, 28.6, 28.7, 33.2, 33.6, 36.7, 51.6, 59.5, 116.1, 118.8, 119.9, 120.4, 129.6, 131.8, 140.2, 146.4, 171.7, 173.7.

7-{3-[1-(4-Nitrophenyl)-1*H*-[1,2,3]triazol-4-yl]phenylcarbamoyl}heptanoic Acid Methyl Ester (3k). Compound **3k** (yield 44%) was prepared from **1** and 1-azido-4-nitrobenzene (**2k**) according to the methodology described for the preparation of compound **3b**. R_f = 0.60 (1:1 hexane/EtOAc). ^{1}H NMR (DMSO-d_6, 500 MHz): δ = 1.31 (br s, 4H), 1.52−1.55 (m, 2H), 1.59−1.62 (m, 2H), 2.29−2.35 (m, 4H), 3.58 (s, 3H), 7.42 (t, *J* = 7.5 Hz, 1H), 7.59 (d, *J* = 6.5 Hz, 2H), 7.93 (t, *J* = 8.0 Hz, 1H), 8.31 (s, 1H), 8.35 (d, *J* = 8.5 Hz, 1H), 8.49 (d, *J* = 8.5 Hz, 1H), 8.82 (s, 1H), 9.53 (s, 1H), 10.03 (s, 1H). ^{13}C NMR (DMSO-d_6, 125 MHz): δ = 24.3, 24.9, 28.2, 28.3, 33.2, 36.3, 51.1, 114.6, 115.9, 119.1, 120.0, 120.2, 123.0, 125.9, 129.3, 130.2, 131.5, 137.2, 139.9, 147.6, 148.5, 171.3, 173.3.

7-{3-[1-(4-Aminophenyl)-1*H*-[1,2,3]triazol-4-yl]phenylcarbamoyl}heptanoic Acid Methyl Ester (3l). A suspension of compound **3l** (0.080 g, 0.17 mmol) and Pd/C (10 wt %, 20 mg) in EtOAc (20 mL) was stirred under hydrogen atmosphere at room temperature for 5 h. The catalyst was removed by filtration through a pad of Celite and washed thoroughly with MeOH. The solvent was evaporated. The residue was purified by column chromatography on silica gel (EtOAc/hexane, 2:1) to give compound **3l** (0.054 g, 72%). R_f = 0.30 (1:1 hexane/EtOAc). ^{1}H NMR (CD_3OD, 500 MHz): δ = 1.40 (br s, 4H), 1.61−1.67 (m, 2H), 1.71−1.75 (m, 2H), 2.34 (t, *J* = 7.5 Hz, 2H), 2.41 (t, *J* = 8.0 Hz, 2H), 3.65 (s, 3H), 4.61 (br s, 2H), 6.81 (d, *J* = 8.0 Hz, 1H), 7.10 (d, *J* = 8.0 Hz, 1H), 7.21 (s, 1H), 7.27 (t, *J* = 8.0 Hz, 1H), 7.41 (t, *J* = 8.0 Hz, 1H), 7.59 (d, *J* = 7.5 Hz, 1H), 7.64 (d, *J* = 7.5 Hz, 1H), 8.11 (s, 1H), 8.74 (s, 1H). ^{13}C NMR (CD_3OD, 125 MHz): δ = 25.8, 26.7, 29.9, 30.0, 34.7, 37.9, 52.0, 107.5, 109.9, 116.4, 118.4, 120.4, 121.2, 122.5, 130.5, 131.4, 132.1, 139.2, 140.5, 149.0, 150.9, 174.7, 176.0.

Octanedioic Acid {3-[1-(4-Fluorophenyl)-1*H*-[1,2,3]triazol-4-yl]phenyl}amide Hydroxyamide (4b). To a solution of hydroxylamine hydrochloride (1.96 g, 28 mmol) in 20 mL of MeOH, KOH (1.58 g, 28 mmol) was added at 40 °C for 10 min. The reaction mixture was cooled to 0 °C and filtered. Compound **3b** (60 mg, 0.14 mmol) was added to the filtrate followed by KOH (0.158 g, 2.8 mmol) at room temperature for 30 min. The reaction mixture was extracted with EtOAc. The organic layer was washed with saturated NH_4Cl aqueous solution and brine, dried over Na_2SO_4, filtered, and concentrated. The residue was purified by preparative HPLC to give compound **4b** (31 mg, 51%). HPLC purity: 14.1 min, 95.6% (method 2). ^{1}H NMR (DMSO-d_6, 400 MHz): δ = 1.29 (br s, 4H), 1.51 (t, *J* = 8.0 Hz, 2H), 1.60 (t, *J* = 8.0 Hz, 2H), 1.94 (t, *J* = 8.0 Hz, 2H), 2.32 (t, *J* = 8.0 Hz, 2H), 7.40 (t, *J* = 8.0 Hz, 1H), 7.49 (t, *J* = 8.0 Hz, 2H), 7.55 (d, *J* = 8.0 Hz, 1H), 7.59 (d, *J* = 8.0 Hz, 1H), 8.01−8.04 (m, 2H), 8.26 (s, 1H), 8.65 (s, 1H), 9.24 (s, 1H), 10.02 (s, 1H), 10.33 (s, 1H). ^{13}C NMR (DMSO-d_6, 100 MHz): δ = 25.4, 28.8, 32.6, 36.8, 116.3, 117.0, 117.3, 171.8, 119.4, 120.3, 120.6, 122.7, 122.8, 129.7, 131.0, 133.6, 140.3, 147.7, 169.5. ESI-HRMS calculated for $[C_{22}H_{24}FN_5O_3 - H]^-$: 424.1790. Found: 424.1790.

Octanedioic Acid Hydroxyamide {3-[1-(4-Iodophenyl)-1*H*-[1,2,3]triazol-4-yl]phenyl}amide (4c). Compound **4c** (yield 27%) was prepared according to the methodology described for the preparation of compound **4b**. HPLC purity: 15.6 min, 95.2% (method 2). ^{1}H NMR (DMSO-d_6, 400 MHz): δ = 1.29 (br s, 4H), 1.50 (t, *J* = 8.0 Hz, 2H), 1.60 (t, *J* = 8.0 Hz, 2H), 1.94 (t, *J* = 8.0 Hz, 2H), 2.33 (t, *J* = 8.0 Hz, 2H), 7.40 (t, *J* = 8.0 Hz, 1H), 7.54−7.60 (m, 2H), 7.81 (d, *J* = 8.0 Hz, 2H), 7.99 (d, *J* = 8.0 Hz, 2H), 8.26 (s, 1H), 8.65 (s, 1H), 9.29 (s, 1H), 10.01 (s, 1H), 10.33 (s, 1H). ^{13}C NMR (DMSO-d_6, 100 MHz): δ = 172.2, 169.8, 148.2, 140.7, 139.4, 137.0, 131.2, 130.1, 122.6, 121.0, 120.3, 119.8, 116.6, 37.1, 33.0, 29.2, 25.8. ESI-HRMS calculated for $[C_{22}H_{24}IN_5O_3 - H]^-$: 532.0851. Found: 532.0849.

Octanedioic Acid Hydroxyamide {3-[1-(4-Trifluoromethylphenyl)-1*H*-[1,2,3]triazol-4-yl]phenyl}amide (4d). Compound **4d** (yield 39%) was prepared according to the methodology described for the preparation of compound **4b**. HPLC purity: 15.6 min, 98.6% (method 2). ^{1}H NMR (DMSO-d_6, 400 MHz): δ = 1.29 (br s, 4H), 1.50 (t, *J* = 8.0 Hz, 2H), 1.60 (t, *J* = 8.0 Hz, 2H), 1.95 (t, *J* = 8.0 Hz, 2H), 2.33 (t, *J* = 8.0 Hz, 2H), 7.42 (t, *J* = 8.0 Hz,

1H), 7.59 (t, J = 8.0 Hz, 2H), 8.03 (d, J = 8.0 Hz, 2H), 8.25 (d, J = 8.0 Hz, 2H), 8.66 (s, 1H), 8.30 (s, 1H), 9.43 (s, 1H), 10.03 (s, 1H), 10.33 (s, 1H). ^{13}C NMR (DMSO-d_6, 100 MHz): δ = 25.4, 28.8, 32.6, 36.8, 116.3, 119.5, 120.2, 120.7, 120.8, 125.8, 127.6, 127.7, 128.9, 129.8, 130.7, 139.8, 140.4, 148.0, 169.5, 171.8. ESI-HRMS calculated for $[C_{23}H_{24}F_3N_5O_3 - H]^-$: 474.1759. Found: 474.1757.

Octanedioic Acid {3-[1-(3,5-Difluorophenyl)-1*H*-[1,2,3]triazol-4-yl]phenyl}amide Hydroxyamide (4e). Compound **4e** (yield 41%) was prepared according to the methodology described for the preparation of compound **4b**. HPLC purity: 15.0 min, 96% (method 2). ^{1}H NMR (DMSO-d_6, 400 MHz): δ = 1.29 (br s, 4H), 1.49 (t, J = 8.0 Hz, 2H), 1.60 (t, J = 8.0 Hz, 2H), 1.94 (t, J = 8.0 Hz, 2H), 2.33 (t, J = 8.0 Hz, 2H), 7.40−7.48 (m, 2H), 7.53−7.59 (m, 2H), 7.86 (d, J = 8.0 Hz, 2H), 8.29 (s, 1H), 8.65 (s, 1H), 9.36 (s, 1H), 10.03 (s, 1H), 10.33 (s, 1H). ^{13}C NMR (DMSO-d_6, 100 MHz): δ = 25.4, 28.8, 32.6, 36.8, 104.1, 104.3, 104.4, 104.6, 116.3, 119.5, 120.3, 120.6, 129.8, 130.6, 138.8, 138.9, 140.4, 148.0, 161.9, 162.1, 164.4, 164.5, 169.5, 171.8. ESI-HRMS calculated for $[C_{22}H_{23}F_2N_5O_3 - H]^-$: 442.1696. Found: 442.1696.

Octanedioic Acid Hydroxyamide {3-[1-(4-Hydroxymethylphenyl)-1*H*-[1,2,3]triazol-4-yl]phenyl}amide (4f). Compound **4f** (yield 45%) was prepared according to the methodology described for the preparation of compound **4b**. HPLC purity: 12.2 min, 95.1% (method 2). ^{1}H NMR (DMSO-d_6, 400 MHz): δ = 1.29 (br s, 4H), 1.50 (t, J = 8.0 Hz, 2H), 1.60 (t, J = 8.0 Hz, 2H), 1.94 (t, J = 8.0 Hz, 2H), 2.33 (t, J = 8.0 Hz, 2H), 4.59 (d, J = 4.0 Hz, 2H), 5.36 (t, J = 8.0 Hz, 1H), 7.40 (t, J = 8.0 Hz, 1H), 7.54−7.61 (m, 4H), 7.93 (d, J = 8.0 Hz, 2H), 8.26 (s, 1H), 8.65 (s, 1H), 9.24 (s, 1H), 10.02 (s, 1H), 10.33 (s, 1H). ^{13}C NMR (DMSO-d_6, 100 MHz): δ = 25.4, 28.8, 32.6, 36.8, 62.6, 116.3, 119.3, 119.9, 120.2, 120.6, 125.8, 128.0, 129.7, 131.1, 135.6, 140.3, 143.7, 147.6, 169.5, 171.8. ESI-HRMS calculated for $[C_{23}H_{27}N_5O_4 - H]^-$: 436.1990. Found: 436.1989.

Octanedioic Acid {3-[1-(3,5-Bis(hydroxymethyl)phenyl)-1*H*-[1,2,3]-triazol-4-yl]phenyl}amide Hydroxyamide (4g). Compound **4g** (yield 43%) was prepared according to the methodology described for the preparation of compound **4b**. HPLC purity: 11.4 min, 95.2% (method 2). ^{1}H NMR (DMSO-d_6, 400 MHz): δ = 1.29 (br s, 4H), 1.50 (t, J = 6.8 Hz, 2H), 1.60 (t, J = 6.4 Hz, 2H), 1.94 (t, J = 7.2 Hz, 2H), 2.32 (t, J = 7.6 Hz, 2H), 4.62 (d, J = 5.6 Hz, 4H), 5.41 (t, J = 6.0 Hz, 2H), 7.38−7.42 (m, 2H), 7.58 (dd, J = 8.0 and 4.0 Hz, 2H), 7.79 (s, 2H), 8.29 (s, 1H), 8.65 (d, J = 4.0 Hz, 1H), 9.27 (s, 1H), 10.01 (s, 1H), 10.33 (s, 1H). ^{13}C NMR (DMSO-d_6, 100 MHz): δ = 25.4, 28.8, 32.6, 36.8, 62.8, 116.3, 116.4, 119.3, 119.9, 120.7, 124.6, 125.8, 129.7, 131.1, 136.9, 140.3, 145.0, 147.6, 169.5, 171.8. ESI-HRMS calculated for $[C_{24}H_{29}N_5O_5 - H]^-$: 466.2096. Found: 466.2095.

Octanedioic Acid {3-[1-(3-Fluoro-4-methoxyphenyl)-1*H*-[1,2,3]-triazol-4-yl]phenyl}amide Hydroxyamide (4h). Compound **4h** (yield 41%) was prepared according to the methodology described for the preparation of compound **4b**. HPLC purity: 14.1 min, 96% (method 2). ^{1}H NMR (DMSO-d_6, 400 MHz): δ = 1.29 (br s, 4H), 1.50 (t, J = 8.0 Hz, 2H), 1.60 (t, J = 8.0 Hz, 2H), 1.94 (t, J = 8.0 Hz, 2H), 2.33 (t, J = 8.0 Hz, 2H), 3.93 (s, 3H), 7.38−7.44 (m, 2H), 7.53 (d, J = 8.0 Hz, 1H), 7.58 (d, J = 8.0 Hz, 1H), 7.79 (d, J = 8.0 Hz, 1H), 7.92 (d, J = 12.0 Hz, 1H), 8.26 (s, 1H), 8.65 (s, 1H), 9.20 (s, 1H), 10.02 (s, 1H), 10.33 (s, 1H). ^{13}C NMR (DMSO-d_6, 100 MHz): δ = 25.0, 25.1, 28.4, 32.3, 36.4, 56.4, 108.7, 108.9, 114.6, 115.9, 116.4, 118.9, 119.7, 120.2, 129.4, 129.6, 130.6, 140.0, 147.3, 150.1, 152.5, 169.1, 171.4. ESI-HRMS calculated for $[C_{23}H_{26}FN_5O_4 + H]^+$: 456.2042. Found: 456.2034.

Octanedioic Acid {3-[1-(4-*tert*-Butylphenyl)-1*H*-[1,2,3]triazol-4-yl]phenyl}amide Hydroxyamide (4i). Compound **4i** (yield 33%) was prepared according to the methodology described for the preparation of compound **4b**. HPLC purity: 16.3 min, 95.5% (method 2). ^{1}H NMR (DMSO-d_6, 400 MHz): δ = 1.30 (br s, 4H), 1.33 (s, 9H), 1.50 (t, J = 8.0 Hz, 2H), 1.60 (t, J = 8.0 Hz, 2H), 1.95 (t, J = 8.0 Hz, 2H), 2.33 (t, J = 8.0 Hz, 2H), 7.40 (t, J = 8.0 Hz, 1H), 7.56 (d, J = 8.0 Hz, 1H), 7.57−7.64 (m, 3H), 7.88 (d, J = 8.0 Hz, 2H), 8.25 (s, 1H), 8.65 (s, 1H), 9.20 (s, 1H), 10.02 (s, 1H), 10.34 (s, 1H). ^{13}C NMR (DMSO-d_6, 100 MHz): δ = 25.4, 28.8, 31.4, 32.6, 34.9, 36.8, 116.3, 119.3, 119.9, 120.1, 120.7, 127.0, 129.7, 131.1, 134.7, 140.3, 147.6, 151.7, 169.5, 171.8. ESI-HRMS calculated for $[C_{26}H_{33}N_5O_3 + H]^+$: 464.2656. Found: 464.2653.

Octanedioic Acid [3-(1-Cyclohexyl-1*H*-[1,2,3]triazol-4-yl)phenyl]amide Hydroxyamide (4j). Compound **4j** (yield 27%) was prepared according to the methodology described for the preparation of compound **4b**. HPLC purity: 7.9 min, 97.4% (method 1). ^{1}H NMR (DMSO-d_6, 400 MHz): δ = 1.20−1.35 (m, 5H), 1.38−1.53 (m, 4H), 1.59 (t, J = 8.0 Hz, 2H), 1.67 (d, J = 12.0 Hz, 1H), 1.78−1.84 (m, 4H), 1.94 (d, J = 8.0 Hz, 2H), 2.09 (d, J = 12.0 Hz, 2H), 2.31 (t, J = 8.0 Hz, 2H), 4.46−4.52 (m, 1H), 7.34 (t, J = 8.0 Hz, 1H), 7.46 (d, J = 8.0 Hz, 1H), 7.55 (d, J = 8.0 Hz, 1H), 8.16 (s, 1H), 8.56 (s, 1H), 9.96 (s, 1H), 10.35 (s, 1H). ^{13}C NMR (DMSO-d_6, 100 MHz): δ = 25.0, 25.1, 25.4, 28.8, 32.6, 33.2, 36.8, 59.6, 116.1, 118.8, 119.8, 120.4, 129.6, 131.8, 140.2, 146.4, 169.5, 171.7. ESI-HRMS calculated for $[C_{22}H_{31}N_5O_3 - H]^-$: 412.2354. Found: 412.2352.

Octanedioic Acid {3-[1-(3-Aminophenyl)-1*H*-[1,2,3]triazol-4-yl]phenyl}amide Hydroxyamide (4l). Compound **4l** (yield 26%) was prepared according to the methodology described for the preparation of compound **4b**. HPLC purity: 10.6 min, 97.1% (method 3). ^{1}H NMR (DMSO-d_6, 400 MHz): δ = 1.28 (br s, 4H), 1.49−1.70 (m, 4H), 1.94 (t, J = 8.0 Hz, 2H), 2.32 (t, J = 8.0 Hz, 2H), 5.58 (br s, 2H), 6.66 (d, J = 8.0 Hz, 1H), 7.00 (d, J = 8.0 Hz, 1H), 7.15 (s, 1H), 7.21 (dd, J = 8.0, 8.0 Hz, 1H), 7.38 (dd, J = 8.0, 8.0 Hz, 1H), 7.54−7.72 (m, 2H), 8.25 (s, 1H), 8.66 (br s, 1H), 9.09 (s, 1H), 10.00 (s, 1H), 10.33 (s, 1H). ^{13}C NMR (DMSO-d_6, 100 MHz): δ = 24.7, 28.1, 31.9, 36.0, 104.5, 106.5, 113.6, 115.5, 118.4, 119.0, 119.9, 128.9, 129.8, 130.4, 137.1, 139.5, 146.7, 149.7, 168.7, 171.0.

7-(3-*tert*-Butoxycarbonylaminophenylcarbamoyl)heptanoic Acid Methyl Ester (6). To a solution of **5** (1.00 g, 4.8 mmol) and suberic acid monomethyl ester (0.903 g, 4.8 mmol) in 15 mL of dry pyridine at 0 °C was added 0.883 g (5.7 mmol) of $POCl_3$ dropwise. This solution was stirred at 0 °C for 1 h, then diluted with EtOAc and washed thoroughly with saturated aqueous $KHSO_4$ and brine, dried over Na_2SO_4, filtered, and concentrated. The residue was purified by column chromatography on silica gel (EtOAc/hexane, 1:3) to give compound **6** (0.847 g, 46%). R_f = 0.55 (1:1 hexane/EtOAc). ^{1}H NMR (DMSO-d_6, 400 MHz): δ = 1.28 (br s, 4H), 1.46−1.55 (m, 13H), 2.24−2.30 (m, 4H), 3.57 (s, 3H), 7.00 (d, J = 8.0 Hz, 1H), 7.11 (t, J = 8.0 Hz, 1H), 7.28 (d, J = 8.0 Hz, 1H), 7.76 (s, 1H), 9.30 (s, 1H), 9.79 (s, 1H). ^{13}C NMR (DMSO-d_6, 100 MHz): δ = 24.7, 25.4, 28.5, 28.6, 28.7, 33.6, 36.7, 79.3, 109.5, 113.5, 129.0, 140.0, 140.1, 153.1, 171.5, 173.7.

7-(3-Aminophenylcarbamoyl)heptanoic Acid Methyl Ester (7). To a solution of compound **6** (0.800 g, 2.1 mmol) in CH_2Cl_2 (15 mL) at 0 °C, TFA (5 mL) was added. After 1 h, the reaction mixture was concentrated in vacuo. The crude product **7** (0.49 g, 83%) was used for the next reaction directly. The analytical sample was purified by preparative thin-layer chromatography (hexanes/EtOAc, 1:1). ^{1}H NMR (DMSO-d_6, 400 MHz): δ = 1.37−1.38 (m, 4H), 1.63−1.67 (m, 2H), 1.68−1.73 (m, 2H), 2.31 (t, J = 7.2 Hz, 4H), 3.67 (s, 3H), 6.43 (d, J = 7.2 Hz, 1H), 6.67 (d, J = 7.2 Hz, 1H), 7.07 (t, J = 7.6 Hz, 1H), 7.20 (s, 1H). ^{13}C NMR (DMSO-d_6, 100 MHz): δ = 24.6, 25.3, 28.7, 33.9, 37.6, 51.5, 106.6, 109.6, 111.0, 129.6, 171.2, 174.2.

7-(3-Azidophenylcarbamoyl)heptanoic Acid Methyl Ester (8). To a solution of **7** (0.450 g, 1.6 mmol) in a 1:3 mixture of acetic acid and water (15 mL) was added $NaNO_2$ (0.446 g, 6.4 mmol) at 0 °C, and the mixture was stirred for 30 min. To this was added NaN_3 (0.420 g, 6.4 mmol) at the same temperature, and stirring was continued for 1 h. To this was added saturated aqueous $NaHCO_3$ solution followed by $NaHCO_3$ powder until the mixture reached about pH 7. The mixture was extracted with EtOAc, and the combined organic extracts were washed with

brine, dried over Na_2SO_4, filtered, and concentrated. The residue was purified by column chromatography on silica gel (EtOAc/hexane, 1:4) to give compound **8** (0.28 g, 56%). R_f = 0.69 (1:1 hexane/EtOAc). ^{1}H NMR (CD_3OD, 400 MHz): δ = 1.38−1.40 (m, 4H), 1.65 (t, J = 6.8 Hz, 2H), 1.70 (t, J = 6.4 Hz, 2H), 2.32−2.39 (m, 4H), 3.65 (s, 3H), 6.79 (d, J = 8.0 Hz, 1H), 7.25−7.33 (m, 2H), 7.50 (d, J = 1.6 Hz, 1H), 9.88 (br s, 1H). ^{13}C NMR (CD_3OD, 100 MHz): δ = 24.1, 25.1, 28.4, 33.2, 36.4, 50.5, 109.9, 113.9, 115.9, 125.8, 129.7, 140.1, 140.5, 173.3, 174.5.

7-[3-(4-Phenyl[1,2,3]triazol-1-yl)phenylcarbamoyl]heptanoic Acid Methyl Ester (10a). In a mixture of **8** (0.12 g, 0.39 mmol) and phenylacetylene (0.06 g, 0.59 mmol) in water and ethyl alcohol (v/v = 1:1, 10 mL), sodium ascorbate (31 mg, 0.15 mmol, dissolved in 1 mL of water) was added, followed by the addition of copper[33] sulfate pentahydrate (19 mg, 0.08 mmol, dissolved in 1 mL of water). The heterogeneous mixture was stirred vigorously overnight at room temperature. The reaction mixture was diluted with EtOAc and washed thoroughly with brine, dried over Na_2SO_4, filtered, and concentrated. The residue was purified by column chromatography on silica gel (hexane/EtOAc, 1:1) to afford 0.078 g (48%) of **10a**. R_f = 0.31 (1:1 hexane/EtOAc). ^{1}H NMR (400 MHz, CD_3OD): δ = 1.31 (br s, 4H), 1.53 (t, J = 8.0 Hz, 2H), 1.60 (t, J = 8.0 Hz, 2H), 2.30 (t, J = 8.0 Hz, 2H), 2.35 (t, J = 8.0 Hz, 2H), 3.57 (s, 3H), 7.39 (t, J = 8.0 Hz, 1H), 7.50 (t, J = 8.0 Hz, 2H), 7.54−7.56 (m, 2H), 7.64 (d, J = 8.0 Hz, 1H), 7.97 (d, J = 8.0 Hz, 2H), 8.36 (s, 1H), 9.26 (s, 1H), 10.22 (s, 1H). ^{13}C NMR (DMSO-d_6, 90 MHz): δ = 172.5, 141.4, 137.6, 131.0, 129.8, 129.0, 126.1, 120.4, 119.7, 115.1, 111.2, 52.0, 37.2, 34.0, 29.1, 29.0, 25.6, 25.1.

7-[3-(4-Cyclohexyl[1,2,3]triazol-1-yl)phenylcarbamoyl]heptanoic Acid Methyl Ester (10b). Compound **10b** (yield 40%) was prepared from **8** and cyclohexylacetylene according to the methodology described for the preparation of compound **10a**. R_f = 0.41 (1:1 hexane/EtOAc). ^{1}H NMR (400 MHz, CD_3OD): δ = 1.40−1.59 (m, 8H), 1.61−1.69 (m, 2H), 1.71−1.80 (m, 3H), 1.86−1.89 (m, 2H), 2.10 (d, J = 12.0 Hz, 2H), 2.34 (t, J = 8.0 Hz, 2H), 2.42 (t, J = 8.0 Hz, 2H), 2.80−2.90 (m, 1H), 3.65 (s, 3H), 7.50−7.60 (m, 3H), 8.22 (s, 1H), 8,26 (s, 1H), 10.07 (br s, 1H). ^{13}C NMR (100 MHz, CD_3OD): δ = 24.7, 25.2, 26.0, 26.1, 28.6, 28.7, 32.8, 33.6, 35.0, 36.7, 51.6, 110.8, 114.6, 118.9, 119.3, 173.7, 130.5, 137.5, 140.9, 153.7, 172.0.

Octanedioic Acid Hydroxyamide [3-(4-Phenyl[1,2,3]triazol-1-yl)phenyl]amide (11a). Compound **11a** (yield 35%) was prepared according to the methodology described for the preparation of compound **4a**. HPLC purity: 13.7 min, 99% (method 2). ^{1}H NMR (DMSO-d_6, 400 MHz): δ = 1.29 (br s, 4H), 1.50 (t, J = 8.0 Hz, 2H), 1.61 (t, J = 8.0 Hz, 2H), 1.94 (t, J = 8.0 Hz, 2H), 2.35 (t, J = 8.0 Hz, 2H), 7.39 (t, J = 4.0 Hz, 1H), 7.48−7.54 (m, 3H), 7.56 (s, 1H), 7.64 (d, J = 8.0 Hz, 1H), 7.97 (d, J = 8.0 Hz, 2H), 8.36 (s, 1H), 8.65 (s, 1H), 9.26 (s, 1H), 10.22 (s, 1H), 10.33 (s, 1H). ^{13}C NMR (DMSO-d_6, 100 MHz): δ = 25.3, 25.4, 28.8, 32.6, 36.8, 110.9, 114.8, 119.3, 120.0, 125.8, 128.6, 129.4, 130.6, 137.3, 147.0, 147.7, 169.5, 172.1. ESI-HRMS calculated for $[C_{22}H_{25}N_5O_3 + H]^+$: 408.2030. Found: 408.2030.

Octanedioic Acid [3-(4-Cyclohexyl-[1,2,3]triazol-1-yl)phenyl]-amide Hydroxyamide (11b). Compound **11b** (yield 30%) was prepared according to the methodology described for the preparation of compound **4a**. HPLC purity: 9.1 min, 96.1% (method 1). ^{1}H NMR (DMSO-d_6, 400 MHz): δ = 1.29 (br s, 4H), 1.40−1.49 (m, 5H), 1.59 (t, J = 8.0 Hz, 2H), 1.68 (d, J = 12.0 Hz, 1H), 1.76 (d, J = 12.0 Hz, 2H), 1.94 (t, J = 8.0 Hz, 2H), 2.01 (d, J = 12.0 Hz, 2H), 2.33 (t, J = 8.0 Hz, 2H), 2.74 (t, J = 8.0 Hz, 1H), 7.47 (d, J = 4.0 Hz, 2H), 7.58 (d, J = 4.0 Hz, 1H), 8.25 (s, 1H), 8.47 (s, 1H), 10.16 (s, 1H), 10.32 (s, 1H). ^{13}C NMR (DMSO-d_6, 100 MHz): δ = 25.3, 25.4, 26.0, 28.8, 32.6, 32.8, 35.0, 36.8, 110.8, 114.6, 118.9, 119.3, 130.5, 137.5, 140.9, 153.7, 169.5, 172.1. ESI-HRMS calculated for $[C_{22}H_{31}N_5O_3 - H]^-$: 412.2354. Found: 412.2357.

7-[3-(1-Phenyl-1*H*-[1,2,3]triazol-4-yl)phenylcarbamoyl]heptanoic Acid (13). To a solution of compound **12** (0.200 g, 0.49 mmol) in a mixture of MeOH (10 mL) and water (10 mL) was added $LiOH \cdot H_2O$ (0.412 g, 9.84 mmol), and the mixture was stirred at room temperature for 1 h. The reaction mixture was acidfied with 1 N HCl dropwise to pH 5 and extracted with EtOAc. The organic layer was washed with water and brine, dried over Na_2SO_4, and then filtered. The solvent was evaporated to give compound **13** (0.172 g, 89%). ^{1}H NMR (DMSO-d_6, 400 MHz): δ = 1.32 (br s, 4H), 1.51 (t, J = 8.0 Hz, 2H), 1.61 (t, J = 8.0 Hz, 2H), 2.20 (d, J = 8.0 Hz, 2H), 2.31 (t, J = 8.0 Hz, 2H), 7.40 (t, J = 8.0 Hz, 1H), 7.52−7.65 (m, 5H), 7.98 (d, J = 8.0 Hz, 2H), 8.26 (s, 1H), 9.26 (s, 1H), 10.01 (s, 1H), 11.92 (br s, 1H). ^{13}C NMR (DMSO-d_6, 100 MHz): δ = 24.8, 25.4, 28.7, 28.8, 34.0, 36.8, 116.3, 119.3, 120.4, 120.7, 129.7, 130.3, 131.0, 137.0, 140.3, 171.7, 174.9. ESI-HRMS calculated for $[C_{22}H_{24}N_4O_3 - H]^-$: 391.1776. Found: 391.1774.

Octanedioic Acid (2-Aminophenyl)amide [3-(1-phenyl-1*H*-[1,2,3]triazol-4-yl)phenyl]amide (14). To a stirred solution of compound **13** (0.1 g, 0.25 mmol) and 1,2-phenyldiamine (0.275 g, 2.54 mmol) in dry DMF (10 mL) at room temperature, HOAt (0.113 g, 0.76 mmol), triethylamine (0.35 mL, 2.54 mmol), and DMAP (0.031 g, 0.25 mmol) were added sequentially. Stirring was continued overnight. The reaction mixture was diluted with ethyl acetate, washed with water, saturated $NaHCO_3$ solution, saturated NH_4Cl solution, and brine, dried over Na_2SO_4, filtered, and concentrated. The crude material was purified by preparative HPLC to give compound **14** (0.042 g, 34%). ^{1}H NMR (DMSO-d_6, 400 MHz): δ = 1.36 (br s, 4H), 1.61−1.63 (m, 4H), 2.29−2.36 (m, 4H), 4.81 (br s, 1H), 6.53 (t, J = 8.0 Hz, 1H), 6.71 (d, J = 8.0 Hz, 1H), 6.88 (t, J = 8.0 Hz, 1H), 7.14 (d, J = 4.0 Hz, 1H), 7.41 (t, J = 8.0 Hz, 1H), 7.50−7.65 (m, 5H), 7.98 (d, J = 8.0 Hz, 2H), 8.27 (s, 1H), 9.09 (s, 1H), 9.26 (s, 1H), 10.03 (s, 1H). ^{13}C NMR (DMSO-d_6, 100 MHz): δ = 25.5, 25.6, 28.9, 36.1, 36.8, 116.3, 116.6, 119.3, 120.4, 120.7, 124.0, 125.7, 125.8, 126.1, 129.1, 129.7, 130.3, 131.0, 137.0, 140.3, 142.3, 147.7, 171.5, 171.8. ESI-HRMS calculated for $[C_{28}H_{30}N_6O_2 + H]^+$: 483.2503. Found: 483.2502.

Biological Methods. HDACs Inhibition Assay. Purified HDACs were incubated with 1 μM carboxyfluorescein (FAM)-labeled acetylated peptide substrate and test compound for 17 h at 25 °C in HDAC assay buffer containing 100 mM HEPES (pH 7.5), 25 mM KCl, 0.1% BSA, and 0.01% Triton X-100. Reactions were terminated by the addition of buffer containing 0.078% SDS for a final SDS concentration of 0.05%. Substrate and product were separated electrophoretically using a Caliper LabChip 3000 system with blue laser excitation and green fluorescence detection (CCD2). The fluorescence intensity in the substrate and product peaks was determined using the Well Analyzer software on the Caliper system. The reactions were performed in duplicate for each sample. IC_{50} values were automatically calculated using the IDBS XLFit, version 4.2.1, plug-in for Microsoft Excel and the XLFit four-parameter logistic model (sigmoidal dose-response model): $A + [(B - A)/1 + (C/x)^D]$, where x is compound concentration, A is the estimated minimum, B is the estimated maximum of % inhibition, C is the inflection point, and D is the Hill slope of the sigmoidal curve. The standard errors of the IC_{50} were automatically calculated using the IDBS XLFit, version 4.2.1, plug-in for Microsoft Excel and the formula xf4_FitResultStdError().

MTS Cell Proliferation Assay. All the pancreatic cancer cell lines were obtained from ATCC (Rockville, MD) and were maintained in a humidified environment at 37 °C with 5% CO_2. BxPc-3 and HupT3 cells were grown in RPMI 1640 (Mediatech, Hercules, CA) containing 10% fetal calf serum (FBS). Panc04.03 was grown in RPMI 1640 medium with 15% FBS. MiaPaca-2 was grown in DMEM (Mediatech, Hercules, CA) with 10% FBS. For cytotoxicity assay, cultured cells were detached with trypsin, washed, and counted. An aliquot ((3−5) × 10^3 cells) was placed in triplicate into 6 wells of a 96-well microtiter plate in a total volume of 150 μL. Four hours after plating, 50 μL of the culture medium containing either

diluent (DMSO) or varying concentrations of the indicated HDACIs from a concentration of 1 nM to 50 μM was added to each well. Cytotoxicity was measured at time 0 and 72 h after treatment using the CellTiter 96 Aqueous Non-Radioactive Cell Proliferation Assay kit (Promega, Madison, WI) according to the manufacturer's instructions. The absorbance of the product formazan, which is considered to be directly proportional to the number of living cells in the culture, was measured at 490 nm using a SpectraMax M2 microplate reader (Molecular Devices, Sunnyvale, CA). The IC_{50} values were calculated using XLfit (IDBS Ltd., Guildford, U.K.).

Xenograft Tumor Model. Female athymic nude mice (8−10 weeks old) were inoculated subcutaneously with 3×10^6 Su86.86 (left flank) and Panc04.03 (right flank) pancreatic cancer cells mixed with Matrigel (BD Biosciences). Two weeks after injection, tumors were size-matched and mice were randomized into three treatment groups: (a) control DMSO, four mice; (b) compound **4a** (10 mg/kg), four mice; (c) compound **4a** (100 mg/kg), four mice. Established SU86.86 and Panc04.03 xenografts (tumor volume 150−200 mm^3) were treated by ip injections with diluent (50 μL DMSO) or compound **4a** (10 and 100 mg/kg every 12 h for 48 h). After cessation of therapy, tumors were dissected from sacrificed animals. Tumor proteins were extracted from fresh tumor tissues taken from mouse, separated by SDS−PAGE (50 μg/well), transferred to polyvinylidene difluoride membrane, and probed with antibodies.

Acknowledgment. This work was supported in part by gift funds from an anonymous donor, by Grant No. 271210 from the ADDF/Elan, and by the Mayo Foundation and the Pancreatic Cancer SPORE P50 CA102701.

References

(1) Butler, K. V.; Kozikowski, A. P. Chemical origins of isoform selectivity in histone deacetylase inhibitors. *Curr. Pharm. Des.* **2008**, *14*, 505–528.

(2) Butler, R.; Bates, G. P. Histone deacetylase inhibitors as therapeutics for polyglutamine disorders. *Nat. Rev. Neurosci.* **2006**, *7*, 784–796.

(3) Jaenisch, R.; Bird, A. Epigenetic regulation of gene expression: how the genome integrates intrinsic and environmental signals. *Nat. Genet.* **2003**, *33*, 245–254.

(4) (a) Grunstein, M. Histone acetylation in chromatin structure and transcription. *Nature* **1997**, *389*, 349–352. (b) Kurdistani, S. K.; Grunstein, M. Histone acetylation and deacetylation in yeast. *Nat. Rev. Mol. Cell Biol.* **2003**, *4*, 276–284. (c) Struhl, K.; Moqtaderi, Z. The TAFs in the HAT. *Cell* **1998**, *94*, 1–4. (d) Wolffe, A. P.; Guschin, D. Review: chromatin structural features and targets that regulate transcription. *J. Struct. Biol.* **2000**, *129*, 102–122.

(5) Bolden, J. E.; Peart, M. J.; Johnstone, R. W. Anticancer activities of histone deacetylase inhibitors. *Nat. Rev. Drug Discovery* **2006**, *5*, 769–784.

(6) Kummar, S.; Gutierrez, M.; Gardner, E. R.; Donovan, E.; Hwang, K.; Chung, E. J.; Lee, M. J.; Maynard, K.; Kalnitskiy, M.; Chen, A.; Melillo, G.; Ryan, Q. C.; Conley, B.; Figg, W. D.; Trepel, J. B.; Zwiebel, J.; Doroshow, J. H.; Murgo, A. J. Phase I trial of MS-275, a histone deacetylase inhibitor, administered weekly in refractory solid tumors and lymphoid malignancies. *Clin. Cancer Res.* **2007**, *13*, 5411–5417.

(7) Kozikowski, A. P.; Chen, Y.; Gaysin, A.; Chen, B.; D'Annibale, M. A.; Suto, C. M.; Langley, B. C. Functional differences in epigenetic modulators—superiority of mercaptoacetamide-based histone deacetylase inhibitors relative to hydroxamates in cortical neuron neuroprotection studies. *J. Med. Chem.* **2007**, *50*, 3054–3061.

(8) Kinzel, O.; Llauger-Bufi, L.; Pescatore, G.; Rowley, M.; Schultz-Fademrecht, C.; Monteagudo, E.; Fonsi, M.; Gonzalez, P. O.; Fiore, F.; Steinkühler, C.; Jones, P. Discovery of a potent class I selective ketone histone deacetylase inhibitor with antitumor activity in vivo and optimized pharmacokinetic properties. *J. Med. Chem.* **2009**, *52*, 3453–3456.

(9) (a) Kelly, W. K.; Richon, V. M.; O'Connor, O.; Curley, T.; MacGregor-Curtelli, B.; Tong, W.; Klang, M.; Schwartz, L.; Richardson, S.; Rosa, E.; Drobnjak, M.; Cordon-Cordo, C.; Chiao, J. H.; Rifkind, R.; Marks, P. A.; Scher, H.; Phase, I clinical trial of histone deacetylase inhibitor: suberoylanilide hydroxamic acid administered intravenously. *Clin. Cancer Res.* **2003**, *9*, 3578–3588. (b) Carducci, M. A.; Gilbert, J.; Bowling, M. K.; Noe, D.; Eisenberger, M. A.; Sinibaldi, V.; Zabelina, Y.; Chen, T. L.; Grochow, L. B.; Donehower, R. C. A phase I clinical and pharmacological evaluation of sodium phenylbutyrate on an 120-h infusion schedule. *Clin. Cancer Res.* **2001**, *7*, 3047–3055. (c) Sasakawa, Y.; Naoe, Y.; Inoue, T.; Sasakawa, T.; Matsuo, M.; Manda, T.; Mutoh, S. Effects of FK228, a novel histone deacetylase inhibitor, on human lymphoma U-937 cells in vitro and in vivo. *Biochem. Pharmacol.* **2002**, *64*, 1079–1090.

(10) (a) Liu, B.; Hong, J. S. Role of microglia in inflammation-mediated neurodegenerative diseases: mechanisms and strategies for therapeutic intervention. *J. Pharmacol. Exp. Ther.* **2003**, *304*, 1–7. (b) Lin, H. S.; Hu, C. Y.; Chan, H. Y.; Liew, Y. Y.; Huang, H. P.; Lepescheux, L.; Bastianelli, E.; Baron, R.; Rawadi, G.; Clâement-Lacroix, P. Anti-rheumatic activities of histone deacetylase (HDAC) inhibitors in vivo in collagen-induced arthritis in rodents. *Br. J. Pharmacol.* **2007**, *150*, 862–872.

(11) (a) Hockly, E.; Richon, V. M.; Woodman, B.; Smith, D. L.; Zhou, X.; Rosa, E.; Sathasivam, K.; Ghazi-Noori, S.; Mahal, A.; Lowden, P. A.; Steffan, J. S.; Marsh, J. L.; Thompson, L. M.; Lewis, C. M.; Marks, P. A.; Bates, G. P. Suberoylanilide hydroxamic acid, a histone deacetylase inhibitor, ameliorates motor deficits in a mouse model of Huntington's disease. *Proc. Natl. Acad. Sci. U.S.A.* **2003**, *100*, 2041–2046. (b) Levenson, J. M.; O'Riordan, K. J.; Brown, K. D.; Trinh, M. A.; Molfese, D. L.; Sweatt, J. D. Regulation of histone acetylation during memory formation in the hippocampus. *J. Biol. Chem.* **2004**, *279*, 40545–40559. (c) Fischer, A.; Sananbenesi, F.; Wang, X.; Dobbin, M.; Tsai, L. H. Recovery of learning and memory is associated with chromatin remodelling. *Nature* **2007**, *447*, 178–182.

(12) Sasakawa, Y.; Naoe, Y.; Noto, T.; Inoue, T.; Sasakawa, T.; Matsuo, M.; Manda, T.; Mutoh, S. Antitumor efficacy of FK228, a novel histone deacetylase inhibitor, depends on the effect on expression of angiogenesis factors. *Biochem. Pharmacol.* **2003**, *66*, 897–906.

(13) (a) Dow, G. S.; Chen, Y. F.; Andrews, K. T.; Caridha, D.; Gerena, L.; Gettayacamin, M.; Johnson, J.; Li, Q.; Melendez, V.; Obaldia, N.; Tran, T. N.; Kozikowski, A. P. Antimalarial activity of phenylthiazolyl-bearing hydroxamate-based histone deacetylase inhibitors. *Antimicrob. Agents Chemother.* **2008**, *52*, 3467–3477. (b) Ouaissi, M.; Ouaissi, A. Histone deacetylase enzymes as potential drug targets in cancer and parasitic diseases. *J. Biomed. Biotechnol.* **2006**, *2006*, 13474.

(14) de Ruijter, A. J.; van Gennip, A. H.; Caron, H. N.; Kemp, S.; van Kuilenburg, A. B. Histone deacetylases (HDACs): characterization of the classical HDAC family. *Biochem. J.* **2003**, *370*, 737–749.

(15) (a) Luo, J.; Nikolaev, A. Y.; Imai, S.; Chen, D.; Su, F.; Shiloh, A.; Guarente, L.; Gu, W. Negative control of p53 by Sir2alpha promotes cell survival under stress. *Cell* **2001**, *107*, 137–148. (b) Marks, P. A.; Richon, V. M.; Miller, T.; Kelly, W. K. Histone deacetylase inhibitors. *Adv. Cancer Res.* **2004**, *91*, 137–168.

(16) Hu, E.; Dul, E.; Sung, C. M.; Chen, Z.; Kirkpatrick, R.; Zhang, G. F.; Johanson, K.; Liu, R.; Lago, A.; Hofmann, G.; Macarron, R.; de los Frailes, M.; Perez, P.; Krawiec, J.; Winkler, J.; Jaye, M. Identification of novel isoform-selective inhibitors within class I histone deacetylases. *J. Pharmacol. Exp. Ther.* **2003**, *307*, 720–728.

(17) Villagra, A.; Cheng, F.; Wang, H. W.; Suarez, I.; Glozak, M.; Maurin, M.; Nguyen, D.; Wright, K. L.; Atadja, P. W.; Bhalla, K.; Pinilla-Ibarz, J.; Seto, E.; Sotomayor, E. M. The histone deacetylase HDAC11 regulates the expression of interleukin 10 and immune tolerance. *Nat. Immunol.* **2009**, *10*, 92–100.

(18) Zhang, C. L.; McKinsey, T. A.; Chang, S.; Antos, C. L.; Hill, J. A.; Olson, E. N. Class II histone deacetylases act as signal-responsive repressors of cardiac hypertrophy. *Cell* **2002**, *110*, 479–488.

(19) Acharya, M. R.; Sparreboom, A.; Venitz, J.; Figg, W. D. Rational development of histone deacetylase inhibitors as anti-cancer agents: a review. *Mol. Pharmacol.* **2005**, *68*, 917–932.

(20) Gao, L.; Cueto, M. A.; Asselbergs, F.; Atadja, P. Cloning and functional characterization of HDAC11, a novel member of the human histone deacetylase family. *J. Biol. Chem.* **2002**, *277*, 25748–25755.

(21) (a) Guo, L.; Han, A.; Bates, D. L.; Cao, J.; Chen, L. Crystal structure of a conserved N-terminal domain of histone deacetylase 4 reveals functional insights into glutamine-rich domains. *Proc. Natl. Acad. Sci. U.S.A.* **2007**, *104*, 4297–4302. (b) Bottomley, M. J.; Lo Surdo, P.; Di Giovine, P.; Cirillo, A.; Scarpelli, R.; Ferrigno, F.; Jones, P.; Neddermann, P.; De Francesco, R.; Steinkühler, C.; Gallinari, P.; Carfí, A. Structural and functional analysis of the human HDAC4 catalytic domain reveals a regulatory structural zinc-binding domain. *J. Biol. Chem.* **2008**, *283*, 26694–26704.

(22) Rivieccio, M. A.; Brochier, C.; Willis, D. E.; Walker, B. A.; D'Annibale, M. A.; McLaughlin, K.; Siddiq, A.; Kozikowski, A. P.; Jaffrey, S. R.; Twiss, J. L.; Ratan, R. R.; Langley, B. HDAC6 is a target for protection and regeneration following injury in the nervous system. *Proc. Natl. Acad. Sci. U.S.A.* **2009**, *106*, 19599–19604.

(23) Zhang, B.; West, E. J.; Van, K. C.; Gurkoff, G. G.; Zhou, J.; Zhang, X. M.; Kozikowski, A. P.; Lyeth, B. G. HDAC inhibitor increases histone H3 acetylation and reduces microglia inflammatory response following traumatic brain injury in rats. *Brain Res.* **2008**, *1226c*, 181–191.

(24) Kozikowski, A. P.; Tapadar, S.; Luchini, D. N.; Kim, K. H.; Billadeau, D. D. Use of the nitrile oxide cycloaddition (NOC) reaction for molecular probe generation: a new class of enzyme selective histone deacetylase inhibitors (HDACIs) showing picomolar activity at HDAC6. *J. Med. Chem.* **2008**, *51*, 4370–4373.

(25) Chen, Y.; Lopez-Sanchez, M.; Savoy, D. N.; Billadeau, D. D.; Dow, G. S.; Kozikowski, A. P. A series of potent and selective, triazolylphenyl-based histone deacetylases inhibitors with activity against pancreatic cancer cells and *Plasmodium falciparum*. *J. Med. Chem.* **2008**, *51*, 3437–3448.

(26) (a) Rostovtsev, V. V.; Green, L. G.; Fokin, V. V.; Sharpless, K. B. A stepwise Huisgen cycloaddition process: copper(I)-catalyzed regioselective "ligation" of azides and terminal alkynes. *Angew. Chem., Int. Ed.* **2002**, *41*, 2596–2599. (b) Tornøe, C. W.; Christensen, C.; Meldal, M. Peptidotriazoles on solid phase: [1,2,3]-triazoles by regiospecific copper(I)-catalyzed 1,3-dipolar cycloadditions of terminal alkynes to azides. *J. Org. Chem.* **2002**, *67*, 3057–3064.

(27) Chen, Y.; He, R.; Chen, Y.; D'Annibale, M. A.; Langley, B.; Kozikowski, A. P. Studies of benzamide- and thiol-based histone deacetylase inhibitors in models of oxidative-stress-induced neuronal death: identification of some HDAC3-selective inhibitors. *ChemMedChem.* **2009**, *4*, 842–852.

(28) Arnold, N. B.; Arkus, N.; Gunn, J.; Korc, M. The histone deacetylase inhibitor suberoylanilide hydroxamic acid induces growth inhibition and enhances gemcitabine-induced cell death in pancreatic cancer. *Clin. Cancer Res.* **2007**, *13*, 18–26.

(29) Kumagai, T.; Wakimoto, N.; Yin, D.; Gery, S.; Kawamata, N.; Takai, N.; Komatsu, N.; Chumakov, A.; Imai, Y.; Koeffler, H. P. Histone deacetylase inhibitor, suberoylanilide hydroxamic acid (vorinostat, SAHA) profoundly inhibits the growth of human pancreatic cancer cells. *Int. J. Cancer* **2007**, *121*, 656–665.

(30) Karagianni, P.; Wong, J. HDAC3: taking the SMRT-N-CoRrect road to repression. *Oncogene* **2007**, *26*, 5439–5449.

(31) Lâopez-Soto, A.; Folgueras, A. R.; Seto, E.; Gonzalez, S. HDAC3 represses the expression of NKG2D ligands ULBPs in epithelial tumour cells: potential implications for the immunosurveillance of cancer. *Oncogene* **2009**, *28*, 2370–2382.

(32) Schneider, G.; Reichert, M.; Saur, D.; Hamacher, R.; Fritsch, R.; Schmid, R. M. HDAC3 is linked to cell cycle machinery in MiaPaCa2 cells by regulating transcription of skp2. *Cell Proliferation* **2007**, *40*, 522–531.

(33) Sanda, T.; Okamoto, T.; Uchida, Y.; Nakagawa, H.; Iida, S.; Kayukawa, S.; Suzuki, T.; Oshizawa, T.; Suzuki, T.; Miyata, N.; Ueda, R. Proteome analyses of the growth inhibitory effects of NCH-51, a novel histone deacetylase inhibitor, on lymphoid malignant cells. *Leukemia* **2007**, *21*, 2344–2353.